Scattering of Ions
VI. Elastic Scattering of N^+ on Ne, Ar, Kr, and Xe

H.-P. Weise und H.-U. Mittmann

Hahn-Meitner-Institut für Kernforschung Berlin GmbH, Bereich Strahlenchemie, Berlin

(Z. Naturforsch. **29 a**, 1143–1151 [1974]; received May 27, 1974)

In the elastic differential cross-section of the N^+-rare gas systems two different types of oscillations have been observed. At an energy of a few eV a primary rainbow was detected for all systems. In the case of N^+-Ar, secondary rainbows were resolved too. From these experimental data the potential depths were determined to be: $\varepsilon(N^+-Ne) = 0.4$ eV, $\varepsilon(N^+-Kr) = 0.29$ eV, $\varepsilon(N^+-Xe) = 0.92$ eV. For the system N^+-Ar the shape of the reduced potential was obtained by evaluating the positions of the secondary rainbow extrema. The potential depth was found to be 2.16 eV.

At higher energies and large scattering angles additional oscillations appeared which are presumed to be Stueckelberg oscillations. For N^+-Ne a single group of strongly marked oscillations appeared up to the highest energies used ($E_L = 220$ eV). In the case of N^+-Ar the amplitudes of these undulations are strongly quenched. For N^+-Kr and N^+-Xe several groups of oscillations with different amplitudes and frequencies seem to be superimposed in the differential cross-section. They are attributed for all systems to crossings of the incoming state with the charge exchanged state.

1. Introduction

During the last few years much attention has been paid to the determination of interaction potentials between ions and neutrals by elastic scattering experiments at energies of a few eV. A knowledge of interaction potentials is an essential condition for the understanding of chemical reactions and the properties of molecules.

In the case of a purely repulsive potential the differential cross-section is a monotonically decreasing function of the scattering angle. If the absolute value of the cross-section can be measured the absolute potential can be determined, either by an inversion procedure [1, 2] or by fitting the parameters of an analytical model potential [3]. If the potential curve has an attractive well the differential cross-section exhibits an oscillatory structure, provided the collision energy is not too high. This so called rainbow structure extends from small angles to a maximum scattering angle. The last maximum is called the primary rainbow; the oscillations at smaller angles secondary rainbows. Beyond the primary rainbow the differential cross-section is monotonic and drops sharply with increasing scattering angle [4–11]. In a high resolution experiment rapid oscillations with a much higher frequency can be observed which are superimposed on the rainbow structure [8]. Their amplitudes decrease sharply on the dark side of the primary rainbow.

Reprint requests to Dr. H.-U. Mittmann, HMI-Strahlenchemie, *D-1000 Berlin 39*, Glienicker Straße 100.

By evaluating the angular positions of the rainbow extrema and of the rapid oscillations the absolute potential can be determined from the minimum to approximately $3\,r_m$ (r_m = equilibrium distance).

The differential cross-section on the dark side of the primary rainbow maximum yields information about the repulsive potential branch which has to be connected to the attractive branch known from the evaluation of the rainbow structure [12].

Oscillations of a different kind called Stueckelberg oscillations may arise if the potential curve under investigation has a crossing (or pseudo-crossing) point with another electronic state of the molecule [13–17]. In most cases the two potential curves cross at small distances, giving rise to oscillations at large values of $\tau = E_c \cdot \vartheta$ (E_c = energy in the centre of mass system, ϑ = scattering angle in the centre of mass system). From the Stueckelberg oscillations information about the excited state may be obtained. Under favourable conditions the evaluation yields the position of the crossing point and the value of the coupling matrix element H_{12}.

In the case of curve crossing inelastic scattering occurs too. If there are crossings between the investigated potential and many other molecular states a great number of scattering events lead into inelastic channels if the energy is sufficiently high. This absorption of intensity from the elastic channel leads to widely spaced undulations in the elastic differential cross-section which can be compared with the wave-optical diffraction pattern behind a light-absorbing disc [14, 17].

2. Experiments

Differential cross-sections for the elastic scattering of N^+-ions on Ne, Ar, Kr, and Xe were measured using the apparatus described previously [8]. The angular spread of the primary ion beam was less than 1.4°, the energy width usually about 0.8 eV FWHM.

In the $N^+ - Ne$ elastic scattering cross-sections a primary rainbow maximum was observed in the lab. energy range $3.5\,\text{eV} < E_L < 9\,\text{eV}$. In some angular distributions the first secondary rainbow could be distinguished but the whole structure was rather shallow. In the energy range from $E_L = 40$ eV to $E_L = 220$ eV a very well pronounced group of Stueckelberg oscillations was detected. Figure 1 shows a typical experimental result for

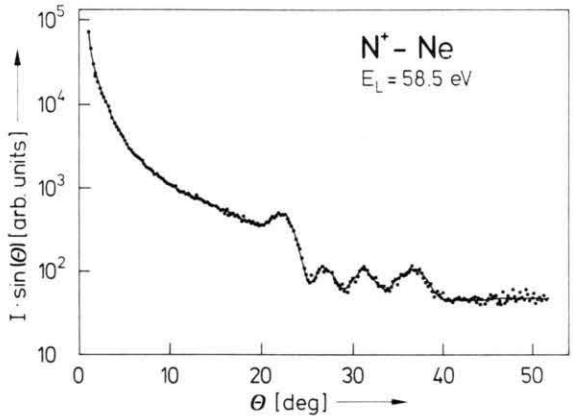

Fig. 1. Differential cross-section for elastic scattering of N^+ by Ne at $E_L = 58.5$ eV.

$E_L = 58.5$ eV. From zero angle up to $\Theta = 20°$ the scattering intensity monotonically decreases and then rises to a first maximum. At larger angles the maximum is followed by a sharp intensity drop and three regular oscillations. For $\Theta > 40°$ no undulations could be detected. At energies $E_L > 100$ eV the minimum between the last two maxima fades (Fig. 2) and at $E_L = 175$ eV (Fig. 3) the two maxima overlap completely giving rise to one maximum of much higher amplitude. For still higher energies this group of oscillations moves to smaller angles without change in structure. Additionally, at large scattering angles a long wavelength undulatory structure with strongly damped amplitudes appears.

In the case of $N^+ - Ar$ a very marked rainbow structure was observed in the energy range $4.5\,\text{eV} < E_L < 40\,\text{eV}$. Between $E_L = 7$ eV and $E_L = 25$ eV up to six secondary rainbow extrema were resolved (Figure 4). At very small scattering angles a further maximum appeared for energies below 12 eV. The energy dependence of the maxima is the same as in the case of a rainbow maximum. For $E_L > 20$ eV Stueckelberg-oscillations were detected at large deflection angles (Figure 5). Thus at inter-

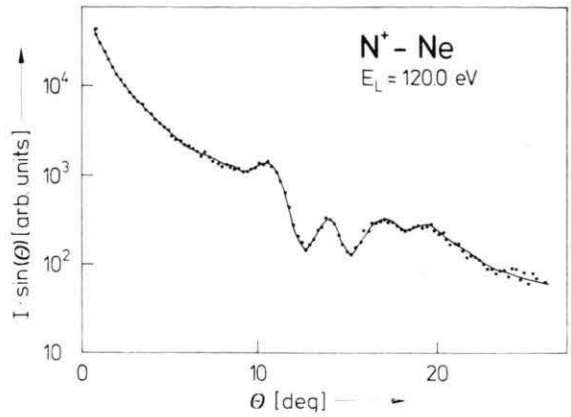

Fig. 2. Differential cross-section for elastic scattering of N^+ by Ne at $E_L = 120.0$ eV.

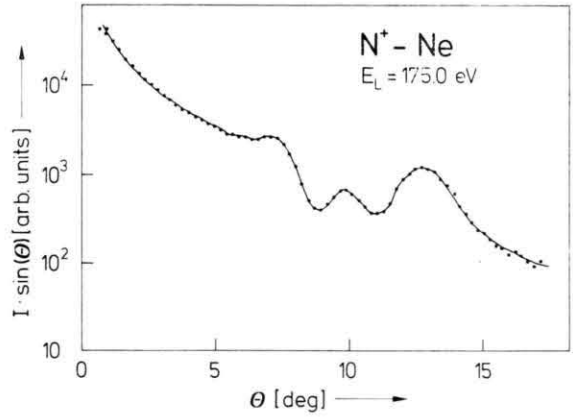

Fig. 3. Differential cross-section for elastic scattering of N^+ by Ne at $E_L = 175.0$ eV.

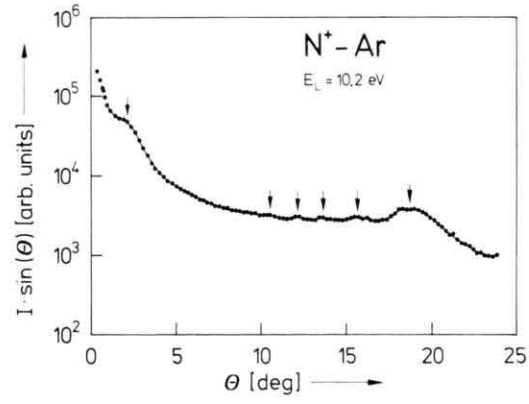

Fig. 4. Differential elastic scattering cross-section for $N^+ - Ar$ at $E_L = 10.2$ eV. The arrows indicate rainbow extrema.

mediate energies the primary and one secondary rainbow can be observed together with the curve-crossing-undulations. The Stueckelberg structure is very similar to that for $N^+ - Ne$ but the amplitudes of the oscillations are markedly damped. At $E_L = 22.5$ eV (Fig. 5) the descent behind the first maximum is less pronounced and the wavelength of the following two oscillations is much longer than for $N^+ - Ne$. At energies $E_L > 70$ eV this structure fades away and a very long wavelength structure appears as in the case of $N^+ - Ne$.

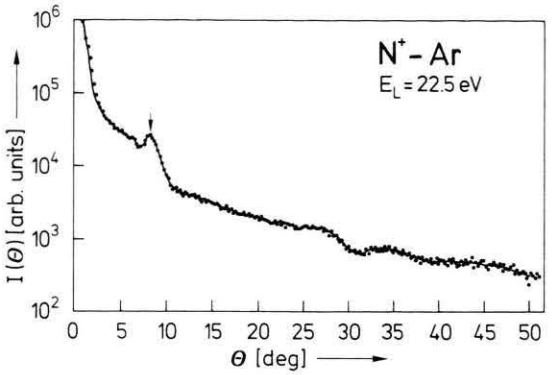

Fig. 5. Differential elastic scattering cross-section for $N^+ - Ar$ at $E_L = 22.5$ eV. The arrow indicates the primary rainbow maximum.

In the differential cross-section for elastic scattering of N^+ by Kr only one primary rainbow extremum appeared in the range $2\,\text{eV} < E_L < 9\,\text{eV}$. For energies $E_L > 20$ eV a complex strongly damped oscillatory structure was detected. In Fig. 6 two different groups of oscillations can be distinguished which might be due to two curve-crossings. At higher energies the pattern becomes even more complicated.

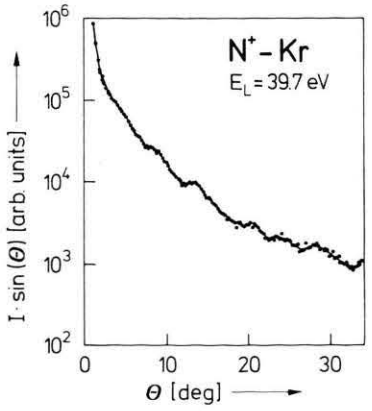

Fig. 6. Differential cross-section for elastic scattering of N^+ by Kr at $E_L = 39.7$ eV.

In Fig. 7 a differential cross-section is plotted for the system $N^+ - Xe$ exhibiting a pronounced rainbow maximum which is indicated by an arrow. Left and right of this extremum further maxima and minima are observed. One of these maxima seems to be superimposed on the rainbow maximum thus giving rise to a higher amplitude of the primary rainbow. At high energies the oscillations are completely damped.

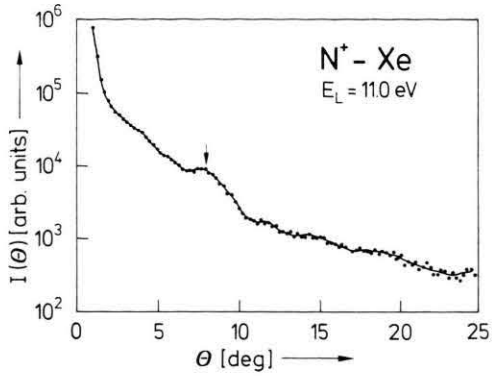

Fig. 7. Differential elastic scattering cross-section for $N^+ - Xe$ at $E_L = 11.0$ eV. The arrow indicates the primary rainbow maximum.

3. Rainbow Structure

Evaluation and Discussion

For the complete determination of the attractive part of the potential curve the rainbow structure with several secondary rainbow maxima and well resolved fine oscillations must be observed. The most detailed experimental information about rainbow structure is available for the $N^+ - Ar$ system. Since the rapid oscillations could not be resolved an independent determination of the potential depth, ε, the equilibrium distance and the shape of the potential curve was not possible. Therefore a reasonable guess was made for the equilibrium distance so that the potential depth and the shape of the attractive well could be evaluated from the measured rainbow structure. This method was chosen since it is easier to make a reasonable guess for r_m than is to guess the shape of the potential curve. Furthermore the potential shape and the depth resulting from the evaluation procedure are not very sensitive to slight variations in the assumed r_m-value. To estimate r_m the value $r_m = 2.43$ Å of the Ar_2^+ molecular ion, taken from a quantum chemical calculation by Gilbert and Wahl [18] was

considered. Since the atomic radius of the N-atom is slightly less than that of the Ar-atom, $r_m(ArN^+) = 2.3$ Å is believed to be a reasonable assumption. The true value is probably within the range $2.0\text{ Å} < r_m < 2.6\text{ Å}$. This uncertainty in the r_m-value gives rise to an a priori uncertainty of $\pm 5\%$ for ε as determined from the measured rainbow structure.

For the evaluation the differential cross-section was calculated wave mechanically for an analytical model potential using JWKB-phases. The potential function was chosen to be of the Morse type:

$$V(r) = \varepsilon\,[\exp\{2\,G_1\,G_2(1 - r/r_m)\} - 2\exp\{G_1\,G_2(1 - r/r_m)\}] \quad (1)$$

with

$$G_2 = 1 \text{ for } r/r_m < 1\,,\ G_2 \neq 1 \text{ for } r/r_m \geqq 1\,.$$

The parameter G_1 determines the shape of the repulsive branch and $G_1 G_2$ that of the attractive one. By varying G_1 which is required for fitting the Stueckelberg oscillations, the shape of the attractive part remains unchanged if the product $G_1 G_2$ is kept constant. For the fit of the rainbow structure G_2 was varied choosing G_1 arbitrarily to be 3.0 (having no influence on the resulting ε-value and the potential shape).

The evaluation procedure was made for a series of energies. At each energy good agreement between the calculated and the measured differential cross-sections was achieved.

The ε-values obtained were found to be slightly energy dependent. This phenomenon is attributed to contact potentials in the ion optical system of the apparatus causing erroneous measurements of the primary ion energy [19]. In order to correct the ε-values, $1/\varepsilon'$ was plotted as a function of $1/E_c'$ according to Equation (2).

$$\frac{1}{\varepsilon'} = \frac{1}{\varepsilon} + \frac{1}{\varepsilon}\,\frac{V_{cc}}{E_c'}\ ; \quad (2)$$

ε' uncorrected potential depth, ε "true" potential depth, V_{CC} contact potential (cm system), E_c' uncorrected c. m. energy following from the measurement.

Figure 8 shows that the plot yields a straight line. ε and V_{CC} are obtained from the intercept and the slope to be

$$\varepsilon = (2.16 \pm 0.15)\text{ eV}, \quad V_c = 0.7\text{ eV (lab. system)}.$$

The form parameter G_2 was found to be $G_2 = 1.3$ (with $G_1 = 3.0$) independent of the energy.

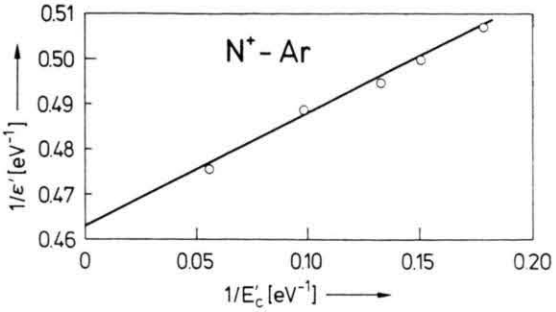

Fig. 8. Plot of the uncorrected reciprocal potential depth versus the uncorrected reciprocal collision energy.

In a prior publication [9] we reported rainbow scattering of protons by Xe-atoms. The resulting potential depths were found to decrease monotonically with increasing collision energy. This effect was attributed to potential curve crossing between the states $H^+ - Xe$ and $H - Xe^+$ [20]. Since for $N^+ - Ar$ ε' increases with increasing energy and Eq. (2) is well obeyed we believe that in this case the energy dependence is due to contact potentials.

The additional maximum at small energies and scattering angles was interpreted as a rainbow maximum. The corresponding potential depth was calculated simply by relating its angular position to that of the main rainbow yielding $\varepsilon = 0.27$ eV.

We suppose that the two rainbows are due to the scattering by two different molecular potentials which are energetically degenerate at infinite separation of N^+ and Ar. According to the Wigner Witmer rules, from the asymptotic state $N^+(^3P^e) + Ar(^1S^e)$ the two molecular states $^3\Sigma^-$ and $^3\Pi$ arise. We assume that the lower lying $^3\Sigma^-$-state is strongly attractive giving rise to the main rainbow structure, whereas the $^3\Pi$-state has only a very small attractive well which causes the rainbow maximum at small angles. Since the projections of the electronic orbital angular momenta of the two states are different, the corresponding scattering amplitudes superimpose incoherently.

Another explanation for the additional rainbow might be that a considerable amount of the primary N^+-ions are in a long-lived metastable state e. g. $2\,s^2\,2\,p^2\,{}^1D^e$ or $2\,s^2\,2\,p^2\,{}^1S^e$.

From these terms molecular states may originate which could be slightly attractive. The scattering intensities from these states can superimpose incoherently on that of the ground state. A further possible explanation of the second rainbow maximum will be discussed below.

For the evaluation of the experimental data of the systems $N^+ - Ne$, Kr, Xe the same procedure was used as for $N^+ - Ar$. Since only primary rainbows were detected for these systems an additional assumption about the shape of the potential curve had to be made. It was thought reasonable to take the experimentally determined reduced potential of $N^+ - Ar$. For the estimation of the equilibrium radii the same considerations were made as for $N^+ - Ar$ giving:

$$r_m(N^+ - Ne) \approx 2.1 \text{ Å},$$
$$r_m(N^+ - Kr) \approx 2.5 \text{ Å}, \quad r_m(N^+ - Xe) \approx 2.8 \text{ Å}.$$

Using these assumptions the wave mechanical fitting procedure was performed. The resulting ε-values were again found to be energy dependent and thus corrected for contact potentials according to the procedure described above. The results are compiled in Table 1.

Table 1. Potential depths determined from rainbow scattering.

System	$N^+ - Ne$	$N^+ - Ar$	$N^+ - Kr$	$N^+ - Xe$
ε [eV]	0.4	2.16 0.27	0.29	0.92

The uncertainty of the quoted values arises from two main sources:

1) the assumption about r_m for $N^+ - Ar$, and the assumption about r_m and the reduced potential for the other systems,
2) the experimental error in the energy measurement and the determination of the angular position of the primary rainbow.

The total error for $N^+ - Ar$ is estimated to be $\pm 7\%$ and for the other systems $\pm 10\%$.

In the case of the H^+- and the He^+-rare gas systems a monotonic increase of the potential depth with increasing atomic number of the rare gas was found. The N^+-rare gas systems on the other hand to do not exhibit such a systematic dependence. $N^+ - Ar$ has a much higher ε than the other systems. This phenomenon might be explained by assuming a crossing between the diabatic $^3\Sigma^-$-ground state of the molecule with the diabatic $^3\Sigma^-$-state originating from the charge exchanged system $N(^4S^o) + Ar^+(^2P^o)$ (Figure 11). This may occur if the $^3\Sigma^-$-curve of the charge exchanged state were strongly attractive (which is suggested by considering the strength of the isoelectronic binding of NCl).

Due to the crossing two different elastic scattering processes may occur.

1. At the crossing point the system follows the adiabatic $^3\Sigma^-$-curve which dissociates into $N^+ + Ar$. The deep potential well of this curve gives rise to the rainbow structure at large angles.
2. The system remains on the weakly attractive diabatic $^3\Sigma^-$-curve originating from $N^+ + Ar$ (nonadiabatic transition). This model implies that the smaller potential depth $\varepsilon = 0.27$ eV for $N^+ - Ar$ must be compared with those of the other systems.

For the other systems this curve crossing model cannot be applied. In the case of $N^+ - Ne$ the charge-exchanged state lies 7 eV higher than the ground state, for $N^+ - Kr$ and $N^+ - Xe$ the charge exchanged states lie 0.53 eV and 2.4 eV respectively below the $N^+ - X$ state (X = noble gas). Therefore a crossing between the incoming state and the charge exchanged state is not expected for these systems.

4. Stueckelberg-oscillations

In the case of rainbow scattering by a non-monotonic potential curve there are generally three impact parameters leading to the same scattering angle. In the wave mechanical picture there is interference between the corresponding partial waves giving rise to oscillations in the differential elastic scattering cross-section. Stueckelberg oscillations however are due to interference between partial waves scattered according to two different potential curves. This situation is shown schematically in Figure 9. The diabatic potential curves $I - II'$ and $II - I'$ cross over at a distance $r = r_c$. If the corresponding electronic wave-functions have the same molecular symmetry the states do not cross in adiabatic approximation. In this case the adiabatic potential curves $I - I'$ and $II - II'$ are said to have a pseudocrossing at $r = r_c$. In the limiting case of the colliding particles having low relative velocities the system follows the adiabatic potential. With increasing relative velocity of the particles at $r = r_c$ there is an increasing probability of a nonadiabatic transition from I to II'. After having reached the classical turning point r_0 the particles may then

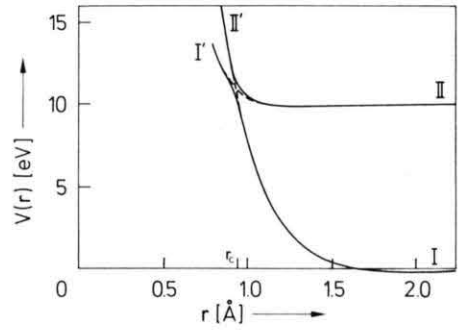

Fig. 9. Schematical representation of a pseudocrossing at $r=r_c$. I−I′ and II−II′ are adiabatic potential curves. I−II′ and II−I′ are the corresponding diabatic curves.

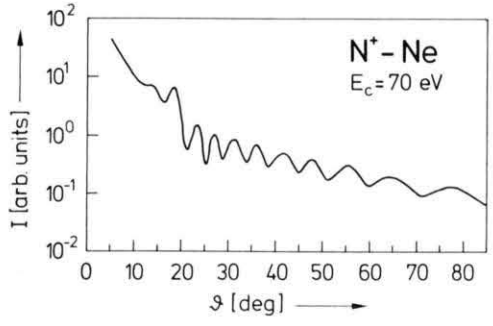

Fig. 10. Differential elastic scattering cross-section for N^+-Ne at $E_c=70$ eV calculated quantum mechanically for the parameters:
a) lower potential: $G_1=4$, $\varepsilon=0.2$ eV, $r_m=2.0$ Å;
b) upper potential: $G_1=5$, $\varepsilon=0.1$ eV, $r_m=1.32$ Å, $H_{12}=0.5$ eV, $\Delta E=10$ eV.

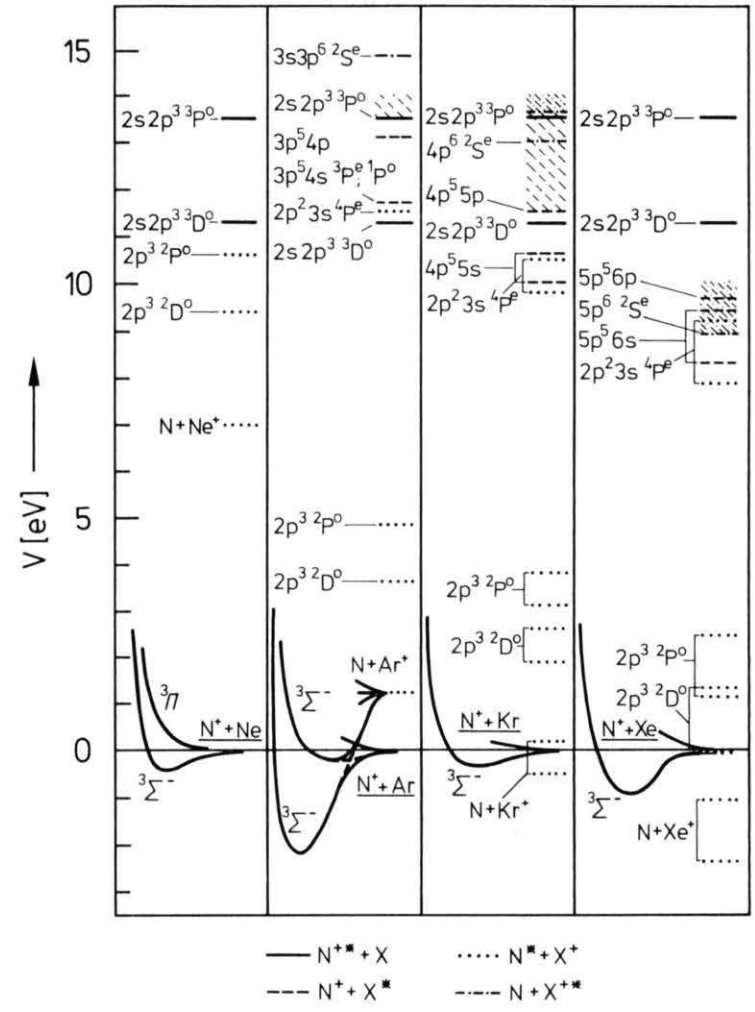

Fig. 11. Energy diagram for the system N^+-Ne, Ar, Kr, and Xe with the asymptotic levels of states yielding $^3\Sigma^-$ and $^3\Pi$ molecular potentials.

follow the adiabatic curve $II' - II$ (inelastic scattering) or may return via a second nonadiabatic transition to I (elastic scattering). There is a second elastic channel which is characterized by adiabatic scattering by the potential $I - I'$ without transition. The scattering amplitudes for the two elastic channels add coherently giving rise to interference oscillations in the differential elastic cross-section. These so-called Stueckelberg oscillations only arise if the distance of closest approach r_0 is smaller than r_c. Therefore the oscillations are only observed beyond a certain value of $\tau = E_c \vartheta > \tau_c$. This critical value τ_c is independent of energy within the range of validity of the small angle approximation.

The analysis of the experimental $N^+ - Ne$ data shows that the τ-values of the leading four extrema of the Stueckelberg oscillations are nearly energy independent in the range $30\,\text{eV} < E_c < 120\,\text{eV}$. Deviation is observed for the last two maxima.

In order to study the influence of the parameters of the two potential curves and the energy dependence of the transition probability, differential cross-sections were calculated quantum mechanically using the following relationships [20–22]:

$$f_{el}(\vartheta) = \frac{1}{2ik} \sum_{l=0}^{\infty} (2l+1)\,(S_l^{el} - 1)\,P_l(\cos\vartheta) \qquad (3)$$

$$S_l^{el} = \exp\{-2\delta_l\} \exp\{2i\eta_l^{I-II'}\} + (1 - \exp\{-2\delta_l\}) \exp\{2i\eta_l^{I-I'}\} \qquad (4)$$

$f_{el}(\vartheta)$	elastic scattering amplitude
k	wave number
l	orbital angular momentum quantum number
$P_l(\cos\vartheta)$	Legendre polynomial
δ_l	transition probability
$\eta_l^{I-II'}$, $\eta_l^{I-I'}$	scattering phases for the two elastic channels

Equation (4) was derived by Stueckelberg [21] assuming that $\delta(I - II') = \delta(II' - I)$. For the calculation of the transition probability the simple Landau-Zener approximation was used [23–25]:

$$\delta_l = \frac{\pi |H_{12}(r_c)|^2}{\hbar\, v_r(r_c) \left| \frac{d}{dr}(H_{11} - H_{22}) \right|_{r=r_c}} . \qquad (5)$$

$H_{12}(r_c)$ is the coupling element, being half the energy difference of the two adiabatic potentials at $r = r_c$

$$v_r(r_c) = \sqrt{\frac{2E_c}{\mu}} \sqrt{1 - \frac{V(r_c)}{E_c} - \frac{b^2}{r_c^2}} , \qquad (6)$$

$v_r(r_c)$ relative radial velocity of the particles at the crossing point r_c, μ reduced mass, b impact parameter, $d(H_{11} - H_{22})/dr$ difference between the slopes of the diabatic potential curves.

To account for the possibility that the potential $I - I'$ might have an attractive well due to the crossing with an attractive potential, instead of the simple JWKB-phases, Miller-phases were used which are still valid if orbiting occurs [26].

For the analytical representation of the two potentials simple Morse functions were used. The potential depth of the ground state curve was taken from the evaluation of the measured rainbow structure. For r_m the estimated value was taken. The form parameter G_1 [Eq. (1)] of the ground state and the parameters ε, r_m, G and ΔE (asymptotic energy) of the excited state were varied. By the choice of these parameters and the collision energy, the value $|d(H_{11} - H_{22})/dr|_{r=r_c}$ and the velocity $v_r(r_c)$ are defined. An additional free parameter is the coupling matrix element H_{12}. The values of r_c, $V(r_c)$, $v_r(r_c)$ and $|d(H_{11} - H_{22})/dr|_{r=r_c}$ are influenced by each of the parameters of both potentials. Due to this coupling the study of the influence of the different parameters is very tedious.

For several combinations of parameters differential cross-sections were obtained which closely resembled the experimental results. A typical curve is shown in Fig. 10 exhibiting the main maximum followed by a steep descent and a series of oscillations with increasing angular separation. The small maximum preceeding the main maximum (Figs. 2 and 3) is also reproduced by the calculation. In contrast to the experimental curves the calculated oscillatory structure continues up to high scattering angles with slightly damped amplitudes. No set of parameters could be found describing equally well all features of the experimental curves. The behaviour of the last two maxima at high energies could not be simulated. This might be due to the insufficient flexibility of the analytical model potentials or to the fact that the right set of parameters could not be found because of limited computer time. Another reason for this failure might be that the use of the simple Landau-Zener-theory is not adequate for a sufficiently precise description of the transition probability [25].

For $N^+ - Ne$ the Stueckelberg-oscillations are very marked in comparison with the other systems. In the

cases of $N^+ - Ar$, Kr, and Xe the amplitudes of the undulations are severely damped and for $N^+ - Kr$ and $N^+ - Xe$ the structures are also more complex. Inspection of the energy diagrams shown in Fig. 11 may be helpful in understanding the observed structures. Zero energy corresponds to the state $N^+ + X$ (X = noble gas atom in the electronic ground state) of the separated particles. The potential depths of the $^3\Sigma^-$-potential curves are as determined from rainbow scattering. For each system the asymptotic energy levels of the lowest lying molecular states are plotted which dissociate either to $N^+ + X^*$ (dashed lines) or to $N^{+*} + X$ (solid lines) or to $N + X^{+*}$ (dashed and dotted lines) or to $N^* + X^+$ (dotted lines). Only states leading to the symmetries $^3\Pi$ and $^3\Sigma^-$ are quoted.

For $(NNe)^+$ the lowest lying excited state has an asymptotic energy of 7 eV. Further states follow above 9 eV. Since for $N^+ - Ne$ the group of Stueckelberg-oscillations is well isolated we suggest that the isolated charge-exchanged state with 7 eV asymptotic energy crosses with the ground state.

In the case of $N^+ - Ar$, Stueckelberg-oscillations are observed approximately at half the τ-values for $N^+ - Ne$ (Figure 5). This agrees with the fact that there are three excited states below 5 eV which are candidates for crossings. For the systems $N^+ - Kr$ and $N^+ - Xe$ even more states are available at energies below 4 eV. Additionally, there are charge-exchanged states below the "incoming" state which may also cross. This large number of possible crossings explains well the complexity of the experimentally observed structure.

In the case of $N^+ - Xe$ oscillations at angles less than the rainbow angle were resolved (Figure 7). They were tentatively interpreted as secondary rainbows and thus used for the determination of the shape of the potential. The fitting procedure however yielded an extremely narrow potential well. Therefore we conclude that the observed maxima are Stueckelberg-oscillations due to a crossing at relatively large distances.

As described above additional oscillations with comparatively long wave-lengths were observed. In the case of $N^+ - Kr$ and $N^+ - Xe$ they are not separated from the first group. Because of the very long wave-lenghts they were tentatively interpreted as diffraction patterns due to strong absorption from the elastic channel. Such oscillations are observed if, at high energies, a sufficient number of curve-crossings lead to strong inelastic scattering [14, 17]. The scattering centre can be compared with an absorbing disc because of the strong reduction of the scattering intensity in the elastic channel. By analogy with wave-optics, the following relationship holds for the angular separation of the extrema of the diffraction pattern:

$$\Delta\vartheta = \pi/k\,a\,, \qquad (7)$$

a: radius of the absorbing disc.

For all systems the periods of the oscillations are approximately constant. The radii were tentatively calculated from Equation (7). For $N^+ - Ne$ the radius of the absorbing disc was found to be $a =$ 0.02 Å and for $N^+ - Ar$ $a = 0.05$ Å. The radii obtained for $N^+ - Kr$ and $N^+ - Xe$ were also about 0.05 Å. These values are more than one order of magnitude smaller than typical atomic dimensions and the radii found by Baudon and others [17]. Therefore we cannot decide whether the long wavelength oscillations are caused by diffraction at the absorbing disc or by a single curve crossing with a highly excited state which does not result in the marked structure as shown in Figure 1.

[1] O. B. Firsov, Zh. Eksper. Teor. Fiz. **24**, 279 [1953].
[2] G. H. Lane and E. Everhart, Phys. Rev. **120**, 2064 [1960].
[3] R. E. Olson, F. T. Smith, and R. C. Mueller, Phys. Rev. **A 1**, 27 [1970].
[4] K. W. Ford and J. A. Wheeler, Ann. Physics (New York) **7**, 259 [1959] and ibid. **7**, 287 [1959].
[5] E. Hundhausen and H. Pauly, Z. Phys. **187**, 305 [1965].
[6] U. Buck and H. Pauly, Z. Phys. **208**, 390 [1968].
[7] D. Beck in: Proceedings of the International School of Physics Enrico Fermi Course XLIV. Molecular Beams and Reaction Kinetics, Academic Press, New York 1970. Editor: Ch. Schlier.
[8] H.-U. Mittmann, H.-P. Weise, A. Ding, and A. Henglein, Z. Naturforsch. **26 a**, 1112 [1971].
[9] H.-P. Weise, H.-U. Mittmann, A. Ding, and A. Henglein, Z. Naturforsch. **26 a**, 1122 [1971].
[10] H.-U. Mittmann, H.-P. Weise, A. Ding, and A. Henglein, Z. Naturforsch. **26 a**, 1282 [1971].
[11] W. G. Rich, S. M. Bobbio, R. L. Champion, and L. D. Doverspike, Phys. Rev. **A 4**, 2253 [1971].
[12] U. Buck, J. Chem. Phys. **54**, 1923 [1971].
[13] F. T. Smith, D. C. Lorents, W. Aberth, and R. P. Marchi, Phys. Rev. Letters **15**, 742 [1965].
[14] F. T. Smith, R. P. Marchi, W. Aberth, and D. C. Lorents, Phys. Rev. **161**, 31 [1967].
[15] D. Coffey, Jr., D. C. Lorents, and F. T. Smith, Phys. Rev. **187**, 201 [1969].
[16] F. T. Smith, H. H. Fleischmann, and R. A. Young, Phys. Rev. **A 2**, 379 [1970].
[17] J. Baudon, M. Barat, and M. Abignoli, J. Phys. **B 3**, 207 [1970].

[18] T. L. Gilbert, and A. C. Wahl, J. Chem. Phys. **55**, 5247 [1971].
[19] H.-P. Weise and H.-U. Mittmann, Z. Naturforsch. **28 a**, 714 [1973].
[20] G.-P. Raabe, Bericht 123, Max-Planck-Institut für Strömungsforschung, Göttingen 1971.
[21] E. C. G. Stueckelberg, Helv. Phys. Acta **5**, 369 [1932].
[22] M. Matsuzawa, J. Phys. Soc. Japan **25**, 1153 [1968].
[23] L. D. Landau, Physik, Z. Sowjetunion **2**, 46 [1932].
[24] C. Zener, Proc. Roy, Soc. London **A 137**, 696 [1932].
[25] E. E. Nikitin in: Chemische Elementarprozesse, Ed. H. Hartmann, J. Heidberg, H. Heydtmann, and G. H. Kohlmaier, Springer-Verlag, Berlin 1968.
[26] W. H. Miller, J. Chem. Phys. **48**, 1651 [1968].